

Fluorescence of Eu^{2+} in Strontium Oxonitridoaluminosilicates (SiAlONs)

Rong-Jun XIE, Naoto HIROSAKI, Yoshinobu YAMAMOTO, Takayuki SUEHIRO,
Mamoru MITOMO and Ken SAKUMA*

Advanced Materials Lab., National Institute for Materials Science (NIMS), 1-1, Namiki, Tsukuba-shi, Ibaraki 305-0044

*Optical Communication Technology Department, Fujikura Ltd., 1440, Mutsuzaki, Sakura-shi, Chiba 285-8550

Eu^{2+} 付活ストロンチウム酸窒化アルミナケイ酸塩（サイアロン）の蛍光特性

解 榮軍・広崎尚登・山本吉信・末廣隆之・三友 護・佐久間 健*

物質・材料研究機構物質研究所, 305-0044 茨城県つくば市並木 1-1

*(株)フジクラ光通信研究部, 285-8550 千葉県佐倉市六崎 1440

The fluorescence of two divalent europium-activated oxonitridoaluminosilicates, namely $\text{SrSi}_5\text{AlO}_2\text{N}_7$ and $\text{SrSiAl}_2\text{O}_3\text{N}_2$, is reported in this work. The powder sample was synthesized by sintering at 1800°C ($\text{SrSi}_5\text{AlO}_2\text{N}_7$) or 1600°C ($\text{SrSiAl}_2\text{O}_3\text{N}_2$) for 2 h under 0.5 MPa N_2 . A single broadband blue-green emission is observed for both $\text{SrSi}_5\text{AlO}_2\text{N}_7 : \text{Eu}^{2+}$ and $\text{SrSiAl}_2\text{O}_3\text{N}_2 : \text{Eu}^{2+}$ at room temperature under ultraviolet excitation. The short-wavelength fluorescence is attributed to the weak crystal-field strength as a result of long distances between the activator ion and ligand anions. The effect of the Eu^{2+} concentration on the emission intensity and CIE chromaticity coordinations of both samples is presented. [Received February 14, 2005; Accepted April 21, 2005]

Key-words: Oxonitridoaluminosilicates, Rare earth, Fluorescence, Phosphor, Concentration quenching, Chromaticity coordination

1. Introduction

An introduction of nitrogen as a substitute for oxygen leads from the oxosilicates to the nitridosilicates ("sions") and, a further partial substitution of Si by Al leads to the oxonitridoaluminosilicates ("sialons"). The extension of the crystal chemistry of oxosilicates has led to the synthesis of a variety of such compounds with potential applications as high performance materials because of their excellent mechanical, thermal, and chemical stability. Typical examples are α -SiAlON [$\text{M}_x(\text{Si}, \text{Al})_{12}(\text{O}, \text{N})_{16}$, M = metal cations and x is the solubility of M] and β -SiAlON [$(\text{Si}, \text{Al})_6(\text{O}, \text{N})_8$] which are derived from α - Si_3N_4 and β - Si_3N_4 , respectively.¹⁻³⁾ Recently, rare-earth activated "sialons" phosphors are gaining considerable importance due to their outstanding luminescence properties and a variety of structural possibilities, which realize potential applications in white light-emitting diodes, fluorescent lamps, and flat panel displays (FPD).⁴⁻¹¹⁾ Krevet et al.⁴⁾ have investigated the significant influence of coordination with N^{3-} on the emission of Ce^{3+} in Y-Si-O-N host lattices. Janssen et al.⁵⁾ reported a novel blue-emitting phosphor $\text{BaAl}_{11}\text{O}_{16}\text{N}$: Eu^{2+} with the β -alumina-type structure, which is suitable for fluorescent lamps. The authors have investigated the luminescence of α -SiAlONs activated by different types of rare earth ions (α -SiAlON:RE, RE = Eu, Tb, or Pr).⁶⁻¹⁰⁾ Among these α -SiAlONs, the Eu^{2+} -doped one shows intense yellow emission upon blue light excitation, and is therefore expected to be used for generating white light when combined with a blue LED chip.^{8),11)}

Extensive studies of alkaline earth silicate and aluminate phosphors have been carried out because of their promising luminescence properties such as high quantum efficiency and good stability.¹²⁻¹⁴⁾ In many cases the emission of Eu^{2+} in alkaline earth silicates and aluminates occurs in the blue region. Recently, alkaline earth silicon nitrides ($\text{M}_2\text{Si}_3\text{N}_8$, M = Ca, Sr, Ba) were reported to give strong red emission when activated with Eu^{2+} .¹⁵⁾ The luminescence of Eu^{2+} in alkaline

earth oxonitridoaluminosilicates, however, is not investigated yet to the best of our knowledge. This triggers the understanding of the emission of Eu^{2+} in these host lattices. Two strontium containing "sialon" compounds, namely $\text{SrSi}_5\text{AlO}_2\text{N}_7$ and $\text{SrSiAl}_2\text{O}_3\text{N}_2$, are recently reported by Shen¹⁶⁾ and Schnick.¹⁷⁾ The crystal structure and cell parameters of these materials are given in Fig. 1 and Table 1, respectively. Both of them have an orthorhombic structure but belong to different space groups. There is only one site for the Sr atoms in both materials. The Sr atoms are located in tunnels extending along [001] in $\text{Sr}_2\text{Si}_{10}\text{Al}_2\text{O}_4\text{N}_{14}$ and in the voids of the $(\text{SiAl}_2\text{O}_3\text{N}_2)^{2-}$ framework in $\text{SrSiAl}_2\text{O}_3\text{N}_2$. As shown in Fig. 2, the Sr atoms are eightfold and ninefold coordinated to (O, N) anions in $\text{SrSi}_5\text{AlO}_2\text{N}_7$ and $\text{SrSiAl}_2\text{O}_3\text{N}_2$, respectively. The Sr-N bond length is much longer than that of the Sr-(O, N) or Sr-O

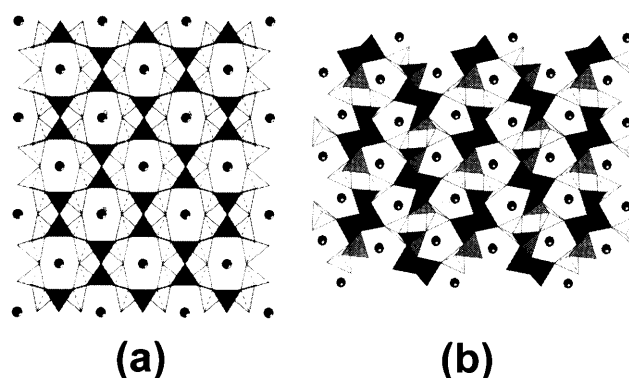
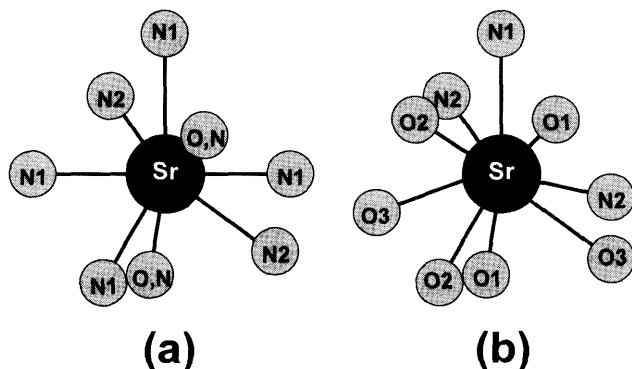


Fig. 1. Crystal structures of (a) $\text{SrSi}_5\text{AlO}_2\text{N}_7$ along [001], Sr atoms are black circles, the Si-(O, N) tetrahedral are dark, and the (Si, Al)-(O, N) ones are unfilled; (b) $\text{SrSiAl}_2\text{O}_3\text{N}_2$ along [100], Sr atoms are black circles, the Si-(O, N) tetrahedral are dark, the Al1-(O, N) ones are grey, and the Al2-(O, N) ones are unfilled.

Table 1. Crystal Structure and Unit Cell Parameters of $\text{SrSi}_5\text{AlO}_2\text{N}_7$ and $\text{SrSiAl}_2\text{O}_3\text{N}_2$

	$\text{SrSi}_5\text{AlO}_2\text{N}_7$	$\text{SrSiAl}_2\text{O}_3\text{N}_2$
Crystal system	orthorhombic	orthorhombic
Space group	Imm2	$P2_12_12_1$
Cell parameter, a	8.2788	4.9198
Cell parameter, b	9.5757	7.8973
Cell parameter, c	4.9158	11.3494
Cell volume, V	389.7	440.94
Z	2	4

Fig. 2. Coordination of Sr atoms in (a) $\text{SrSi}_5\text{AlO}_2\text{N}_7$ and (b) $\text{SrSiAl}_2\text{O}_3\text{N}_2$.

bonds in both materials.

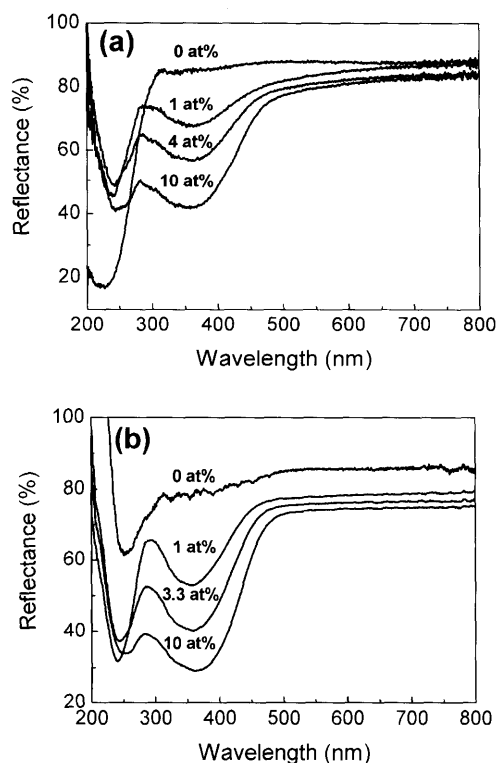
This paper investigates the luminescence properties of europium doped $\text{SrSi}_5\text{AlO}_2\text{N}_7$ and $\text{SrSiAl}_2\text{O}_3\text{N}_2$ at room temperature, and discusses the influence of surroundings in the lattice (e.g., coordination, bond length between Eu and the nearest ligands) and activator concentration on the Eu^{2+} luminescence.

2. Experimental

Powder samples of $\text{SrSi}_5\text{AlO}_2\text{N}_7 : \text{Eu}^{2+}$ and $\text{SrSiAl}_2\text{O}_3\text{N}_2 : \text{Eu}^{2+}$, with the europium concentration varying in the range of 0.5–10 at% with respect to strontium, were prepared from $\alpha\text{-Si}_3\text{N}_4$ (SN-E10, Ube Industries Ltd.), AlN (Tokuyama Corp., Type F), SrCO_3 (Kojundo Chemical Laboratory Co., Ltd.), SiO_2 (Kojundo Chemical Laboratory Co., Ltd.) and Eu_2O_3 (Shin-Etsu Chemical Co., Ltd.). The powder mixtures were synthesized by sintering at 1800°C ($\text{SrSi}_5\text{AlO}_2\text{N}_7 : \text{Eu}^{2+}$) or 1600°C ($\text{SrSiAl}_2\text{O}_3\text{N}_2 : \text{Eu}^{2+}$) for 2 h under 0.5 MPa N_2 . The photoluminescence spectra were measured at room temperature using a fluorescent spectrophotometer (F-4500, Hitachi Ltd.) with a 150 W Ushio xenon short arc lamp. The emission spectrum was corrected for the spectral response of a monochromator and Hamamatsu R928P photomultiplier tube by a light diffuser and tungsten lamp (Noma, 10 V, 4 A). The excitation spectrum was also corrected for the spectral distribution of the xenon lamp intensity by measuring rhodamine-B as reference. The diffusive reflection spectrum was recorded in the range of 200–800 nm on a UV-VIS spectrophotometer with an integrating sphere (JASCO; Ubest V-560).

3. Results and discussion

Figure 3 shows the diffuse reflectance spectra of $\text{SrSi}_5\text{AlO}_2\text{N}_7 : \text{Eu}^{2+}$ and $\text{SrSiAl}_2\text{O}_3\text{N}_2 : \text{Eu}^{2+}$ at room temperature. The spectra of these samples resemble each other in the range of 200–800 nm. Both samples have two absorption bands in

Fig. 3. Diffuse reflectance spectra of (a) $\text{SrSi}_5\text{AlO}_2\text{N}_7$ and (b) $\text{SrSiAl}_2\text{O}_3\text{N}_2$ with varying Eu^{2+} concentration.

the UV spectral region, which are situated at ~ 240 and ~ 360 nm, respectively. Note that the first band is caused by the absorption of the host lattice and the second one by the absorption of Eu^{2+} . With increasing the europium concentration, the absorption becomes stronger and the onset of the absorption band shifts to longer wavelengths for both samples. The reflectance spectra of the concentrated samples extend to the visible part of the spectrum, which yields green daylight color for both samples.

The excitation and emission spectra of $\text{SrSi}_5\text{AlO}_2\text{N}_7 : \text{Eu}^{2+}$ and $\text{SrSiAl}_2\text{O}_3\text{N}_2 : \text{Eu}^{2+}$ are illustrated in Fig. 4. Both samples give blue-green luminescence upon 305 nm excitation. The emission spectrum shows a broad-band character, centered at 488 and 475 nm for $\text{Sr}_2\text{Si}_{10}\text{Al}_2\text{O}_4\text{N}_{14}$ and $\text{SrSiAl}_2\text{O}_3\text{N}_2$, respectively. The emission band corresponds to the allowed $4f^65d \rightarrow 4f^7$ electronic transitions of Eu^{2+} . In comparison with $\text{SrSiAl}_2\text{O}_3\text{N}_2$, $\text{SrSi}_5\text{AlO}_2\text{N}_7$ covers more green and red emissions and has a larger full width of half emission maximum (103 nm) than that of $\text{SrSiAl}_2\text{O}_3\text{N}_2$ (78 nm). Meanwhile, both samples absorb strongly in the range of 350–400 nm, so they can be well excited by a GaN-based UV LED, allowing them to be used for white LED applications as blue phosphors.

The excitation spectra of both samples are broad and structureless and correspond to the $4f^7 \rightarrow 4f^65d$ transition of Eu^{2+} . The broad excitation band is situated at 311 and 305 nm for $\text{SrSi}_5\text{AlO}_2\text{N}_7 : \text{Eu}^{2+}$ and $\text{SrSiAl}_2\text{O}_3\text{N}_2 : \text{Eu}^{2+}$, respectively. No distinct splitting of the 5d band of Eu^{2+} is observed in both samples, suggesting the interaction between the crystal field and the 5d configuration is weak. In addition, the serious spectral overlap also results in an unresolved spectrum. The excitation spectra are consistent with the reflection spectra, and have a tail extending to 460 nm which explains the green color of the powder. For different monitoring wavelengths

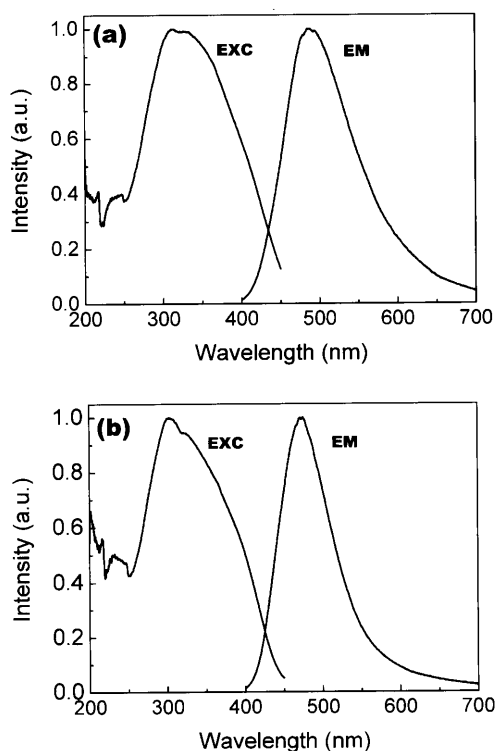


Fig. 4. Excitation and emission spectra of (a) $\text{SrSi}_5\text{AlO}_2\text{N}_7$ and (b) $\text{SrSiAl}_2\text{O}_3\text{N}_2$ with the Eu^{2+} concentration of 1.0 at%.

(450–600 nm), the shape of the excitation spectra does not change. This also holds true for the emission spectra when excited under varying wavelengths (250–400 nm). The presence of one type of excitation and emission spectra is expected as only one crystallographic Sr^{2+} site is present in both samples.

Compared to $\text{Ca-}\alpha\text{-SiAlON}:\text{Eu}^{2+}$ ^(6,8,9) and $(\text{Ca}, \text{Sr}, \text{Ba})_2\text{Si}_5\text{N}_8:\text{Eu}^{2+}$ ⁽¹⁵⁾ the luminescence of $\text{SrSi}_5\text{AlO}_2\text{N}_7$ and $\text{SrSiAl}_2\text{O}_3\text{N}_2$ occurs at shorter wavelength (i.e., higher energy), but resembles that of $\text{BaAl}_{11}\text{O}_{16}\text{N}:\text{Eu}^{2+}$ which emits at 450 nm under UV excitation. The short emission wavelength in $\text{BaAl}_{11}\text{O}_{16}\text{N}:\text{Eu}^{2+}$ is due to the fact that europium is not coordinated to nitrogen, making it similar to the luminescence of Eu-doped barium aluminate phase I.⁽⁵⁾ Li et al. reported that $\text{SrYSi}_4\text{N}_7:\text{Eu}^{2+}$ has a longer emission wavelength than $\text{BaYSi}_4\text{N}_7:\text{Eu}^{2+}$, and ascribed this to smaller metal-ligand distances in SrYSi_4N_7 .⁽¹⁸⁾ As shown in Fig. 2, in $\text{SrSi}_5\text{AlO}_2\text{N}_7$ the Sr atoms are coordinated by eight (O, N) atoms: two (O, N) atoms at 0.2660 nm, two N2 atoms at 0.3219 nm and four N1 atoms at 0.3189 nm;⁽¹⁶⁾ In $\text{SrSiAl}_2\text{O}_3\text{N}_2$ the Sr atoms are coordinated by six O atoms and three N atoms: two O1 at 0.2807 nm, two O2 at 0.2634 nm, two O3 at 0.2887 nm, two N1 at 0.3114 nm and one N2 at 0.2874 nm.⁽¹⁷⁾ The average Sr-(O, N) distance in $\text{SrSi}_5\text{AlO}_2\text{N}_7$ (0.3064 nm) or $\text{SrSiAl}_2\text{O}_3\text{N}_2$ (0.2862 nm) is longer than that observed in $\text{Ca-}\alpha\text{-SiAlON}$ (0.2606 nm) and $\text{Ca}_2\text{Sr}_3\text{N}_8$ (0.2652–0.2708 nm). The Eu^{2+} luminescence greatly depends on the strength of the crystal field. The crystal field increases with decreasing distance between Eu^{2+} and ligand anions and with increasing valence. The long distance between Eu and (O, N) atoms in present materials is thought to cause weak crystal field acting on Eu^{2+} , which results in the short emission wavelength of $\text{SrSi}_5\text{AlO}_2\text{N}_7$ and $\text{SrSiAl}_2\text{O}_3\text{N}_2$. In addition, the coordination of the Eu atoms in $\text{SrSiAl}_2\text{O}_3\text{N}_2$ is oxygen-rich, resulting in weak nephelauxetic effect in comparison with nitride phosphors where Eu^{2+} is

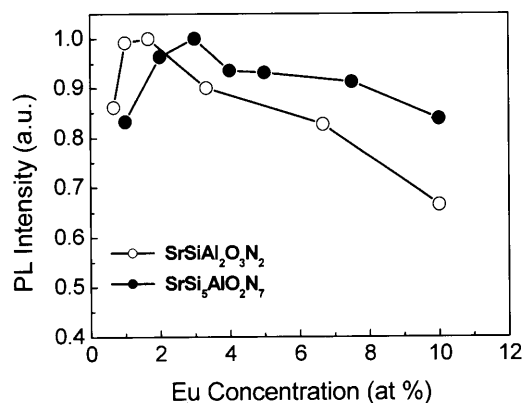


Fig. 5. Concentration dependence of emission intensity of $\text{SrSi}_5\text{AlO}_2\text{N}_7$ and $\text{SrSiAl}_2\text{O}_3\text{N}_2$.

coordinated to nitrogen. This also explains the short emission wavelength of Eu^{2+} in $\text{SrSiAl}_2\text{O}_3\text{N}_2$.

Figure 5 shows the europium concentration dependence of the emission intensity. The critical concentration is 2 and 3 at% for $\text{SrSi}_5\text{AlO}_2\text{N}_7$ and $\text{SrSiAl}_2\text{O}_3\text{N}_2$, respectively. The decrease in emission intensity beyond a critical concentration can be explained by concentration quenching which is mainly caused by the energy transfer between Eu^{2+} ions. Since the $4f \rightarrow 5d$ transition of Eu^{2+} is allowed and the luminescence spectrum overlaps at 400–470 nm, the nonradiative energy transfer among Eu^{2+} ions take places as a result of an electric multipolar interaction and radiation reabsorption. When the concentration of Eu^{2+} increases, the distance between Eu^{2+} ions becomes small, the probability of energy transfer thus increases.⁽¹⁹⁾ Furthermore, the spectral overlap between the emission and excitation spectra leads to energy transfer, which also accounts for concentration quenching.

As allowed electric-dipole transitions are involved in the case of Eu^{2+} , the value of the critical energy transfer distance (R_c) between Eu^{2+} ions can be determined from the following equation⁽²⁰⁾

$$R_c^6 = 0.63 \times 10^{28} \times \frac{4.8 \times 10^{-16} P}{E^4} S.O. \quad (1)$$

Here P is the oscillator strength of the involved absorption transition of the Eu^{2+} ion, E the energy of maximum spectral overlap, and $S.O.$ the spectral overlap integral. For P , a value of 10^{-2} for the broad $4f^7$ to $4f^65d^1$ absorption band is taken.⁽²¹⁾ E and $S.O.$ can be derived from the spectral data. Taking $E = 2.85$ eV ($\text{SrSi}_5\text{AlO}_2\text{N}_7$) and 2.92 eV ($\text{SrSiAl}_2\text{O}_3\text{N}_2$) and $S.O. = 0.044$ ($\text{SrSi}_5\text{AlO}_2\text{N}_7$) and 0.036 ($\text{SrSiAl}_2\text{O}_3\text{N}_2$) into Eq. (1), the critical distance (R_c) value of energy transfer between the Eu^{2+} and the Eu^{2+} ions is estimated to be 1.65 and 1.57 nm for $\text{SrSi}_5\text{AlO}_2\text{N}_7$ and $\text{SrSiAl}_2\text{O}_3\text{N}_2$, respectively.

In addition, the critical concentration can be used to compute the critical energy transfer distance by using the following equation:⁽²²⁾

$$R_c = 2 \left(\frac{3V}{4\pi x_c N} \right)^{1/3} \quad (2)$$

Here x_c is the critical concentration, N the number of cation sites in the unit cell, and V the volume of the unit cell. The critical distance for energy transfer is determined to be 2.10 and 1.91 nm for $\text{SrSi}_5\text{AlO}_2\text{N}_7$ and $\text{SrSiAl}_2\text{O}_3\text{N}_2$, respectively. As seen, there is a good agreement between the R_c values obtained from the experimental spectral data (Eq. (1)) and the crystal

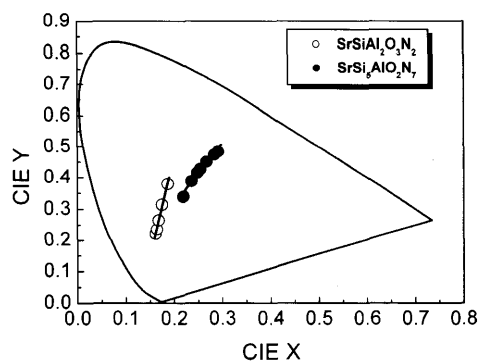


Fig. 6. CIE chromaticity coordinates of $\text{SrSi}_5\text{AlO}_2\text{N}_7$ and $\text{SrSiAl}_2\text{O}_3\text{N}_2$ with varying Eu^{2+} concentration. The Eu^{2+} concentration increases from bottom (0.5 at%) to top (10 at%).

structure data (Eq. (2)).

Figure 6 shows the CIE chromatic coordinates of both samples with varying europium concentration. It is observed that with increasing Eu concentration, the color shifts from blue to bluish-green. This result can be explained by the shift of the emission towards longer wavelength as the Eu^{2+} concentration increases. The red-shift of the emission is perhaps due to some changes in the crystal field around Eu^{2+} which causes the splitting of 5d electrons. As mentioned previously, the probability of the energy transfer from the Eu^{2+} ions at higher levels of 5d to those at the lower levels of 5d increases with an increase of Eu concentration. This makes it possible that higher Eu concentration lowers the emission energy for transfer from the low 5d excited state to the 4f ground state, and hence shifts the emission to longer wavelength. In addition, reabsorption of the highest energy emission occurs in concentrated samples, due to a spectral overlap between the lowest energy excitation band and the highest energy emission. This also leads to an upward shift of the emission maximum to longer wavelengths.

4. Conclusions

The fluorescence of $\text{SrSi}_5\text{AlO}_2\text{N}_7$ and $\text{SrSiAl}_2\text{O}_3\text{N}_2$ activated by divalent europium was investigated at room temperature. Unlike α -SiAlON and alkaline earth silicon nitride, both $\text{SrSi}_5\text{AlO}_2\text{N}_7$ and $\text{SrSiAl}_2\text{O}_3\text{N}_2$ are characteristic of short-wavelength excitation and emission. It is perhaps due to the weak crystal field strength caused by longer distances between Eu^{2+} and ligand anions. The concentration quenching occurs at the Eu^{2+} concentration of 2 and 3 at% for $\text{SrSi}_5\text{AlO}_2\text{N}_7$ and $\text{SrSiAl}_2\text{O}_3\text{N}_2$, respectively. With increasing Eu^{2+} concentration

the CIE chromatic coordinates increase, shifting the color of both samples from blue to blue-green.

Acknowledgement We are grateful to the referee for his/her comments on the manuscript.

References

- 1) Hampshire, S., Park, H. K., Thompson, D. P. and Jack, K. H., *Nature* (London), Vol. 274, pp. 880-882 (1978).
- 2) Cao, G. Z. and Metselaar, R., *Chem. Mater.*, Vol. 3, pp. 242-252 (1991).
- 3) Ekstrom, T. and Nygren, M., *J. Am. Ceram. Soc.*, Vol. 75, pp. 259-276 (1992).
- 4) Krevel, J. W. H., Hintzen, H. T., Metselaar, R. and Meijerink, A., *J. Alloys Compd.*, Vol. 268, pp. 272-277 (1998).
- 5) Jansen, S. R., Migchels, J. M., Hintzen, H. T. and Metselaar, R., *J. Electrochem. Soc.*, Vol. 146, pp. 800-806 (1999).
- 6) Xie, R.-J., Mitomo, M., Uheda, K., Xu, F.-F. and Akimune, Y., *J. Am. Ceram. Soc.*, Vol. 85, pp. 1229-1234 (2002).
- 7) Xie, R.-J., Hirosaki, N., Mitomo, M., Yamamoto, Y., Suehiro, T. and Ohashi, N., *J. Am. Ceram. Soc.*, Vol. 87, pp. 1368-1370 (2004).
- 8) Xie, R.-J., Hirosaki, N., Sakuma, K., Yamamoto, Y. and Mitomo, M., *Appl. Phys. Lett.*, Vol. 84, pp. 5404-5406 (2004).
- 9) Xie, R.-J., Hirosaki, N., Mitomo, M., Yamamoto, Y., Suehiro, T. and Sakuma, K., *J. Phys. Chem. B*, Vol. 108, pp. 12027-12031 (2004).
- 10) Xie, R.-J., Hirosaki, N., Yamamoto, Y., Suehiro, T., Xu, X. and Mitomo, M. (unpublished).
- 11) Sakuma, K., Omichi, K., Kimura, N., Ohashi, M., Tanaka, D., Hirosaki, N., Yamamoto, Y., Xie, R.-J. and Suehiro, T., *Opt. Lett.*, Vol. 29, pp. 2001-2003 (2004).
- 12) Blasse, G., Wanmaker, W. L., Ter Vrugt, J. W. and Bril, A., *Philips Res. Rep.*, Vol. 23, pp. 189-200 (1968).
- 13) Blasse, G. and Bril, A., *Philips Res. Rep.*, Vol. 23, pp. 201-206 (1968).
- 14) Yamazaki, K., Nakabayashi, H., Kotera, Y. and Ueno, A., *J. Electrochem. Soc.*, Vol. 133, pp. 657-660 (1986).
- 15) Hoppe, H. A., Lutz, H., Morys, P., Schnick, W. and Seilmeier, A., *J. Phys. Chem. Solids.*, Vol. 61, pp. 2001-2006 (2000).
- 16) Shen, Z., Grins, J., Esmailzadeh, S. and Ehrenberg, H., *J. Chem. Mater.*, Vol. 9, pp. 1019-1022 (1999).
- 17) Lauterbach, R. and Schnick, W., *Z. Anorg. All. Chem.*, Vol. 624, pp. 1154-1158 (1998).
- 18) Li, Y. Q., Fang, C. M., De With, G. and Hintzen, H. T., *J. Solid State*, Vol. 177, pp. 4687-4694 (2004).
- 19) Qiu, J., Miura, K., Sugimoto, N. and Hirao, K., *J. Non-Cryst. Solids*, Vol. 213-214, pp. 266-268 (1997).
- 20) Blasse, G., *Philips Res. Repts.*, Vol. 24, pp. 131-144 (1969).
- 21) Blasse, G., *J. Solid State Chem.*, Vol. 62, pp. 207-211 (1986).
- 22) Van Uitert, L. G., *J. Electrochem. Soc.*, Vol. 114, pp. 1048-1053 (1967).